Mem. S.A.It. Vol. 1, 1
© SAIt 2008

Memorie della

arXiv:1010.6024v2 [astro-ph.CO] 29 Oct 2010

Demography of obscured and unobscured AGN: prospects for a Wide Field X-ray Telescope

R. Gilli[1], P. Tozzi[2], P. Rosati[3], M. Paolillo[4], S. Borgani[2,5], M. Brusa[6], A. Comastri[1], E. Lusso[7], F. Marulli[7], C. Vignali[7], and the WFXT team

[1] INAF – Osservatorio Astronomico di Bologna, Via Ranzani 1, I-40127 Bologna, Italy
e-mail: `roberto.gilli@oabo.inaf.it`
[2] INAF – Osservatorio Astronomico di Trieste, Via Tiepolo 11, I-34131 Trieste, Italy
[3] ESO, Karl Schwarzschild Strasse 2, 85748 Garching bei Muenchen, Germany
[4] Università Federico II, Dip. di Scienze Fisiche C.U. Monte S.Angelo, ed.6, via Cintia 80126, Napoli
[5] Dip. di Astronomia dell'Università di Trieste, Via G.B. Tiepolo 11, I-34131 Trieste, Italy
[6] MPE, Giessenbachstrasse, 1, 85748 Garching bei Muenchen, Germany
[7] Dip. di Astronomia, Università di Bologna, Via Ranzani 1, 40127 Bologna, Italy

Abstract. We discuss some of the main open issues in the evolution of Active Galactic Nuclei which can be solved by the sensitive, wide area surveys to be performed by the proposed Wide Field X-ray Telescope mission.

Key words. Galaxies: active – X-rays; Active Galactic Nuclei – galaxies: high-redshift

1. Introduction

The observed scaling relations between the structural properties of massive galaxies (bulge mass, luminosity, and stellar velocity dispersion) and the mass of the black holes (BHs) at their centers suggest that galaxy assembly and black hole growth are closely related phenomena. This is often referred to as BH/galaxy co-evolution. The BH growth is thought to happen primarily through efficient accretion phases accompanied by the release of kinetic and radiative energy, part of which can be deposited into the galaxy interstellar medium. Active Galactic Nuclei (AGN) are then believed to represent a key phase across a galaxy's lifetime. Support for this hypothesis comes from several lines of evidence such as i) the match between the mass function of BHs grown through AGN phases and that observed in local galaxies (Marconi et al. 2004; Shankar et al. 2004); ii) the cosmological "downsizing" of both nuclear activity and star formation (Ueda et al. 2003; Cowie et al. 1996); iii) the feedback produced by the AGN onto the galaxy interstellar medium through giant molecular outflows (Feruglio et al. 2010). A number of semi-analytic models (SAMs) have been proposed over about the past decade to explain the BH/galaxy co-evolution (Kauffmann & Haehnelt 2000; Monaco et al. 2007; Menci et al. 2008; Marulli et al. 2008; Lamastra et al. 2010). These models follow the evolution and growth of dark matter structures

---

Send offprint requests to: R. Gilli

across cosmic time, either through the Press-Schechter formalism or through N-body simulations, and use analytic recipes to treat the baryon physics within the dark matter halos. A common assumption of these models is that mergers between gas-rich galaxies trigger nuclear activity and star formation. Recently, a BH/galaxy evolutionary sequence associated to "wet" galaxy mergers has been proposed (Hopkins et al. 2008), in which an initial phase of vigorous star formation and obscured, possibly Eddington limited, accretion is followed by a phase in which the nucleus first gets rid of the obscuring gas shining as an unobscured QSO, then quenches star formation, and eventually fades, leaving a passively evolving galaxy.

While being successful in many respects, this picture is still very partial and many fundamental pieces are missing to get a satisfactory understanding of BH/galaxy co-evolution, such as the very first stages of this joint evolution (e.g. at redshifts $z > 6$), the cosmological evolution of nuclear obscuration, the triggering mechanisms and environmental effects of nuclear activity. In this contribution it will be shown how the proposed Wide Field X-ray Telescope mission (WFXT) can effectively address some of these fundamental issues through sensitive, large area X-ray surveys.

2. The WFXT surveys at a glance

As detailed in Rosati et al. (2010, this volume), WFXT is a mission thought and designed to perform X-ray surveys, featuring a large (1 deg^2) field-of-view (FOV), large (1 m^2 at 1 keV) effective area, and sharp (5" HEW) resolution, constant across the FOV (the quoted values refer to the goal mission design). The observational survey strategy with WFXT will consist of three main X-ray surveys with different area and depth to sample objects in a wide range of redshifts and luminosities. To illustrate the power of the WFXT surveys, a simple excercise can be performed by rescaling the number of X-ray sources obtained from well-known X-ray surveys of similar sensitivity. The 20000 deg^2 WFXT-Wide survey will cover about 2000 times the area of the XBootes survey (Murray et al. 2005), in which more than 3000 X-ray sources have been detected, with the same depth. Similarly, the 3000 deg^2 WFXT-Medium and 100 deg^2 WFXT-Deep surveys will cover 3000 times the area of the C-COSMOS survey (Elvis et al. 2009) and 1000 times the area of the 2Ms CDFS survey (Luo et al. 2008), in which 1700 and 450 objects have been detected, respectively. By summing these numbers it is easy to see that the total source sample obtained by WFXT, mainly composed by AGN, will contain more than 10 million objects.

A more precise estimate of the number of AGN to be detected is obtained by considering the logN-logS relationships in the soft, 0.5-2 keV, and hard, 2-7 keV, bands. About 15 millions AGN detections are expected in the soft band up to $z > 6$ and about 4 millions in the hard band. Remarkably, for a very large number of objects it would be possible to obtain an accurate spectral characterization over the 0.5-7 keV WFXT band pass and derive physical properties such as the X-ray absorption (see Section 4 and Matt & Bianchi, 2010, this volume). Indeed, it is worth noting that, while being most effective at 1 keV, the WFXT collecting area at > 4 keV is still significantly large: in the goal design, the effective area at 5 keV is equal to that of XMM (pn+2MOS combined) at the same energy.

In the following Sections we will present a few unique science cases which can be addressed only with wide area and sensitive X-ray surveys.

3. Supermassive Black Holes in the early Universe

Most stars formed at $0.5 < z < 3$, when SMBHs were also growing most of their mass, but the assembly of the first organized structures started at earlier epochs, as soon as baryons were able to cool within dark matter halos. Discovering the first galaxies and black holes ever formed and understanding how their (concurrent?) formation takes place is a fascinating subject to which more and more efforts will be devoted in the next decade. To date, several tens of galaxies and about 20 QSOs have been confirmed spectroscopically at redshifts above 6 (e.g. Taniguchi 2008; Fan 2006; Willott et al. 2009). Besides a GRB discovered at $z \sim 8.2$ (Salvaterra et al. 2009; Tanvir et al. 2009) and a galaxy at $z = 8.6$ (Lehnert et al. 2010), no other object is known spectroscopically at $z > 7$, although more than 100 galaxy candidates have been recently isolated through deep near-IR imaging with WFC3 (Oesch et al. 2010; Wilkins et al. 2010). The most distant SMBHs known to date are three QSOs at $z \sim 6.4$ discovered through the SDSS (Fan 2006) and the CFHQS survey (Willott et al. 2009, 2010). These two surveys have been the main resource for investigating the most distant QSOs in the past decade. About 20 QSOs at $z > 5.7$ have been detected in the SDSS main survey, which represent the brightest tail of the early QSO population ($\log L_x \sim 45.5$; $\log L_{bol} \sim 47$). Less luminous objects have been detected in the SDSS deep stripe (Jiang et al. 2009) and CFHQS. The BH masses measured for the SDSS bright objects are of the order of $10^9\ M_\odot$ (Kurk et al. 2007, 2009), which must have been built in less than 1 Gyr, i.e. the age of the Universe at $z = 6$. These giant black holes are thought to have formed through mass accretion onto smaller seeds with mass ranging from $10^2 M_\odot$, as proposed for the remnants of massive, PopIII stars (Madau & Rees 2001), to $10^4 M_\odot$, as proposed for the products of direct collapse of large molecular clouds (Volonteri et al. 2008). Whatever the seed origin is, to account for the observed BH mass distribution at $z \sim 6$, BH growth must have proceeded almost continuously at (or even above) the Eddington limit for a time interval of about 1 Gyr. Recent hydrodynamical simulations have shown that, within large dark matter halos, merging between proto-galaxies at $z \sim 14$ with seed BH masses of $10^4 M_\odot$ may trigger Eddington limited nuclear activity to produce a 10^9 solar mass BH by $z \sim 6$ (Li et al. 2007). The overall frequency and efficiency by which this merging and fueling mechanism can work is however unknown.

Because of the paucity of observational constraints, the study of BH and galaxy formation at early epochs remained speculative. For example, the relation between the BH mass and the galaxy gas mass has been measured for a few bright QSOs at $z \sim 5-6$, in which the ratio between the BH mass and the dynamical mass within a few kpc radius, as measured from CO line observations, is of the order of 0.02-0.1 (Walter et al. 2004). This is more than one order of magnitude larger than the ratio between the BH mass and stellar bulge mass measured in local galaxies. Despite the uncertainties on these measurements (see e.g. Narayanan et al. 2008), the possibility that SMBHs are leading the formation of the bulge in proto-galaxies, poses severe constraints to galaxy formation models. Large statistical samples of $z > 6$ AGN are needed to understand the relation between the BH growth and formation of stars in galaxies at their birth. Based on SAMs (see e.g. Hopkins et al. 2008 and Marulli et al. 2008 for recent works), the luminosity function and spatial distribution (clustering) of AGN at $z > 6$ would constrain: i) where, i.e. in which dark matter halos, they form; ii) what their average accretion rate is; iii) what the triggering mechanism (e.g. galaxy interactions vs secular processes) is.

The accreting SMBHs at $z > 6$ known to date have been all selected as *i*-band dropouts ($i - z \gtrsim 2$) in optical surveys. The sky density of the bright ($z_{AB} < 20.2$) QSOs at $z > 6$ in the SDSS main survey is 1/470 deg^2. Fainter objects ($z_{AB} \sim 21 - 22$) have densities of 1 every ~30-40 deg^2 (Jiang et al. 2009; Willott et al. 2009). The discovery of significant samples of objects therefore relies on the large areas covered by these surveys (>8000 deg^2 for the SDSS, ~900 deg^2 for the CFHQS). Based on the SDSS and CFHQS samples, a few attempts to measure the luminosity function of $z \sim 6$ QSOs have been performed, the most recent of which are those by Jiang et al. (2009) and Willott et al. (2010). While the uncertainties at low luminosities ($M_{1450} > -25$) are still substantial, the space density of luminous QSOs ($M_{1450} < -26.5$; $L_{bol} > 10^{47}$ erg s^{-1}) is relatively well constrained, decreasing exponentially from $z \sim 3$ to $z \sim 6$ (see Fig. 1). Furthermore, multiwavelength studies of SDSS QSOs at $z \sim 6$ showed that these objects have metallicities and spectral energy distributions pretty similar to those of lower red-

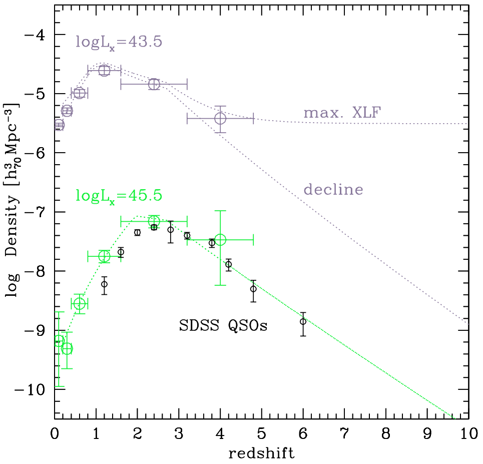

Fig. 1. The space density of unabsorbed AGN with $\log L_x = 43.5$ and $\log L_x = 45.5$. Big open circles are from Hasinger et al. (2005). Small black symbols have been obtained from the space density of optically luminous SDSS QSOs (Richards et al. 2006) by assuming $\alpha_{ox} = -1.5$. The space density of luminous QSOs is found to decrease from $z \sim 3$ to $z \sim 6$ and is well fitted by an exponential decline curve (dotted line from Gilli et al. 2007). The space density of lower luminosity objects is unconstrained for $z > 4$, and we show two alternative working hypotheses: either a "decline" scenario, as observed for luminous QSOs, or a constant density model, which is referred to as "maximum XLF".

shifts QSOs, suggesting their are already mature objects in a young Universe (see however Jiang et al. 2010 for two counter-examples).

Most of the multiwavelength studies mentioned above refer to optical QSOs above the knee of the luminosity function. These likely represent a minor fraction of the active BH population at $z > 6$, which is expected to be made primarily by less massive, $\approx 10^6\ M_\odot$, and less luminous, 10^{44} erg s^{-1}, objects.

When compared with optically selected objects at the same redshift, X-ray selected AGN are on average less luminous, either intrinsically or because of obscuration effects. Therefore X-ray selection might be the key to sample the bulk of the high-z AGN population. Several arguments indeed suggest that obscured AGN should be abundant even at very high redshift. First, observations and modeling showed that obscured AGN outnumber unobscured ones by a significant factor up to $z \lesssim 4$ and it is then reasonable to extrapolate that even at $z > 6$. Second, most current models of galaxy formation postulate that the early phases of accretion onto seed black holes are obscured (e.g. Menci et al. 2008). Third, optical/near-IR spectroscopy and IR/sub-mm imaging of $z \sim 6$ QSOs showed that dust and metals are abundant in their inner regions (Juarez et al. 2009; Beelen et al. 2006). Dust and metals must have then formed in large quantities at $z > 6$ and can effectively absorb the nuclear radiation from the optical regime to the soft X-rays.

Among the objects discovered so far at $z > 6$ no one is obscured, since these have been selected only through optical color selection criteria. The most distant object discovered to date through X-ray selection is an AGN at $z = 5.4$ in the COSMOS field (Civano et al. in preparation) and only a few are known at $z > 4$. The lack of sufficient sky area covered to deep sensitivities is the reason behind that. The discovery space for early obscured AGN is therefore huge, and can have a significant impact on our understanding of BH and galaxy formation.

Different routes can be tried to estimate the space and surface density of X-ray emitting high-z AGN and hence make forecasts for the samples to be observed in the WFXT surveys. As a first step, we considered extrapolations based on our current knowledge of the AGN X-ray luminosity function (XLF) and evolution. As shown in Fig. 1, the space density of luminous, unobscured QSOs with $M_{1450} < -26.5$ has been determined to steadily decrease from $z \sim 3$ to $z \sim 6$ (Richards et al. 2006). When their optical luminosity is converted to the X-rays (using $\alpha_{ox} = -1.5$), there is a good match between their space density and that determined by Hasinger et al. (2005) for soft X-ray selected QSOs in the overlapping redshift range. The behaviour of lower luminosity sources, $\log L_x = 43.5$, is instead known only up to $z \sim 4$ (Yencho et al. 2009; Aird et al. 2010) and extrapolations to higher redshifts are highly uncertain (see Brusa et al. 2010, this

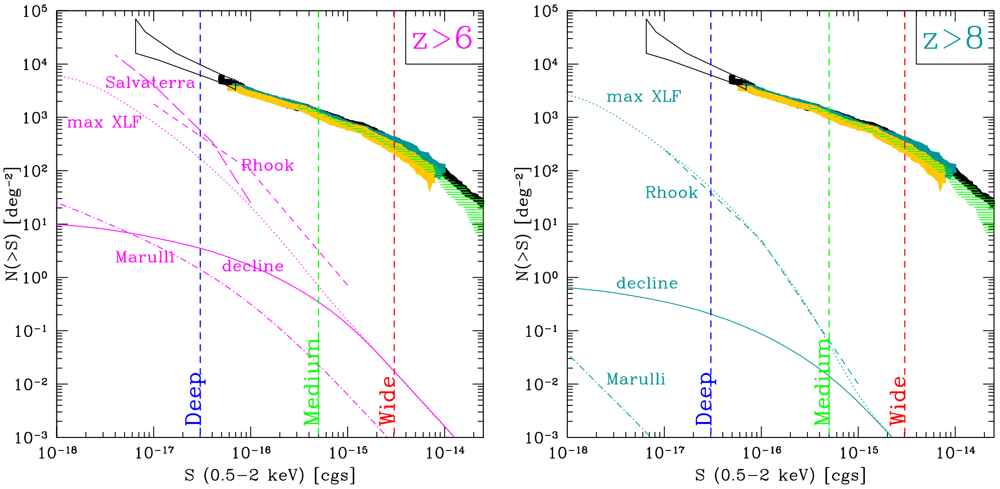

Fig. 2. *Left:* Expected number counts in the 0.5-2 keV band for $z > 6$ AGN according to different models as labeled (see text for details). The datapoints and shaded regions show the observed, total logN-logS of X-ray sources. The sensitivity limits of the three WFXT surveys are shown as vertical dashed lines. *Right*: As in the *left* panel but for $z > 8$ AGN.

volume). Starting from the X-ray background synthesis model by Gilli et al. (2007), we considered a first scenario in which the space density of AGN with $\log L_x < 44$ undergoes the same exponential decline as observed for luminous QSOs - which we will call the “decline” scenario - and a second, perhaps extreme, scenario in which it stays constant above a redshift of ~ 4, which will be referred to as the “maximum XLF” scenario (see Fig. 1). The 0.5-2 keV logN-logS of $z > 6$ AGN expected in the two above mentioned scenarios is shown in Fig. 2, where we also show a range of predictions based on different SAMs of BH/galaxy coevolution (Salvaterra et al. 2007; Rhook & Haehnelt 2008; Marulli et al. 2008). The limiting fluxes of the three WFXT surveys are also shown. It is clear how the $z > 6$ AGN Universe is a completely uncharted territory, the various predictions differing by a few orders of magnitude already at fluxes around 10^{-16} cgs. The predictions by the SAMs of Salvaterra et al. (2007) and Rhook & Haehnelt (2008) are even more optimistic than the “maximum XLF” scenario, predicting about 500-600 $z > 6$ AGN deg^{-2} at the WFXT-Deep limiting flux. The model by Marulli et al. (2008) is instead the most pessimitic, with 15 $z > 6$ AGN deg^{-2} at the same limiting flux. The predictions by SAMs depend on a pretty large number of parameters such as the mass of seed BHs, their location in the density field (i.e. the abundance of the dark matter halos hosting them), the recipes used for accretion, the AGN lightcurve. Although different assumptions are made by different models, the ~ 3 orders-of-magnitude difference at faint X-ray fluxes between the predictions by Marulli et al. (2008) on the one hand, and Salvaterra et al. (2007) and Rhook & Haehnelt (2008) on the other hand, seems to be primarily related to the assumed space density of seed black holes. In the Marulli et al. (2008) model, seed BHs are placed in each halo that can be resolved by the Millennium simulation, i.e. in those halos with mass above $\sim 10^{10}$ $M_{\odot}$, while in Salvaterra et al. (2007) BHs populate minihalos with mass as low as $\sim 10^{7-8}$ $M_{\odot}$, which are therefore much more abundant. In Rhook & Haehnelt (2008) BHs are assumed to radiate at the Eddington limit and their mass to be proportional to that of the hosting halos. This implies that, if small mass seed are assumed, these populate low mass, abundant ha-

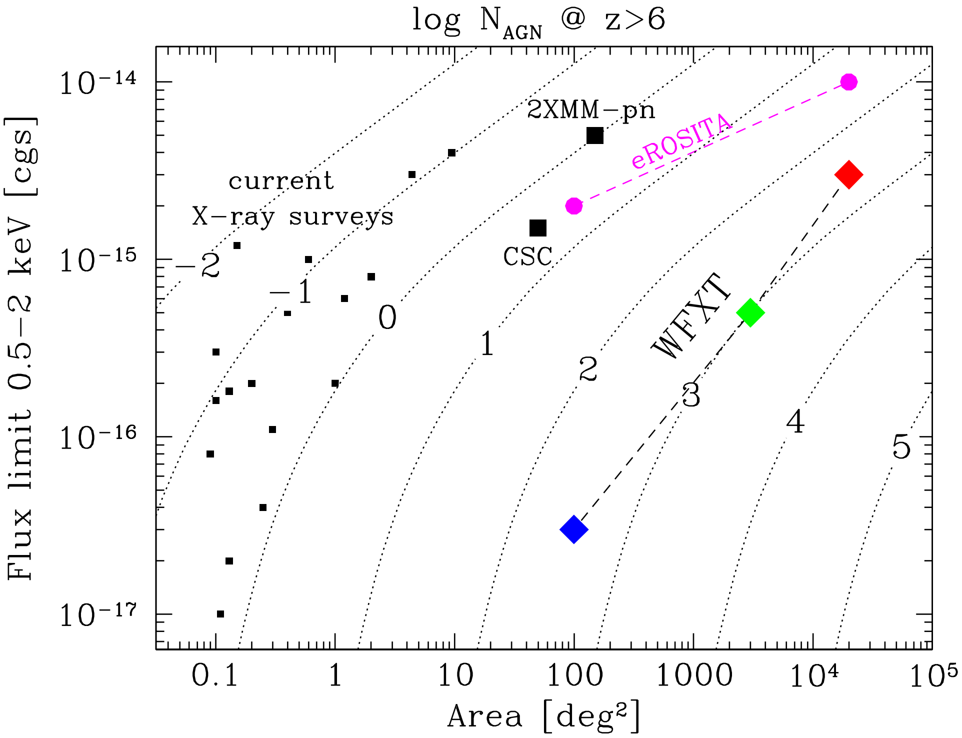

Fig. 3. *Left:* Number of AGN at $z > 6$ expected from the "decline" model (see text) for different combination of survey area vs 0.5-2 keV limiting flux. Dotted lines are the locii of equal AGN number as labeled (labels are in log units). Small black squares show the major Chandra and XMM surveys (either performed or ongoing, including the 4Ms CDFS, the 2Ms CDFN, C-COSMOS, AEGIS, XBootes and many others). Big black squares show the current coverage of the Chandra (CSC) and XMM (2XMM-pn) archives. The deep and wide surveys to be performed with eROSITA in 4 years are shown as magenta circles (based on Cappelluti et al. 2010, this volume). The three WFXT surveys (5 year program) are shown as rotated squares. Less than one $z > 6$ AGN is expected in each of the current X-ray surveys. eROSITA will return about 40 objects with the current design. WFXT will detect about 1600 objects.

los. If large mass seeds are assumed, these populate less abundant halos but their luminosity, and hence detectability, is higher. In each case, surface densities as high as 500 deg^{-2} at the WFXT-Deep limiting flux are reached.

Observations of significant samples at $z > 6$ would constrain the physics of early BH formation disentangling between these scenarios. The surveys performed by WFXT have the power to provide such large statistical samples. As a reference model, we will consider the "decline" model outlined above, which is found to be in excellent agreement with the 0.5-2 keV logN-logS of AGN at $z > 3, 4, 5$ (Brusa et al. 2009, Civano et al. in prep.). About 1600 AGN at $z > 6$ are expected to be detected by WFXT, and about 70 ot them should be at $z > 8$. A summary of the predictions for AGN at $z > 6$ and $z > 8$ in the three WFXT surveys for the decline and maximum XLF scenarios is shown in Table 1. In the WFXT-Deep survey it will be possible to detect in significant numbers $z > 6$ AGN down to $\log L_x = 43.1$ and $z > 8$ AGN down to $\log L_x = 43.4$, making possible to determine the shape of the high-z XLF. To compare the high-z AGN yields from WFXT surveys with what is expected from major current X-ray surveys and with other X-ray mis-

Table 1. Number and minimum 0.5-2 keV luminosity of high-z AGN expected in the WFXT surveys according to the two evolution models (“decline” and “max LF”) described in the text.

Quantity	Survey		
	Deep	Medium	Wide
$z > 6$			
$\log L^{min}$(0.5-2 keV)	43.1	44.3	45.1
N. AGN (decline)	300	1000	300
N. AGN (max LF)	15000	2300	300
$z > 8$			
$\log L^{min}$(0.5-2 keV)	43.4	44.6	45.4
N. AGN (decline)	20	45	10
N. AGN (max LF)	4300	210	10

sions which are either proposed or planned, we show in Fig. 3 the number of $z > 6$ AGN to be detected with different combination of surveyed sky area and soft limiting flux according to the “decline” scenario. It is evident that even the major current X-ray surveys (e.g. CDFS, CDFN, COSMOS, AEGIS, X-Bootes) should return less than one object per field. In the full Chandra and XMM archives (labeled as CSC and 2XMM-pn, respectively) one would expect less than 10 objects in total. With the current mission design and survey strategy (Cappelluti et al. 2010, this volume), the eROSITA satellite, planned for launch in 2012, is expected to return about 40 $z > 6$ AGN, most of them at the luminosities of bright SDSS QSOs. The big leap is clearly expected to be performed by WFXT. The mission design and observing strategy studied for the Internation X-ray Observatory (IXO) are still uncertain: IXO will probably return a sample of $z > 6$ AGN with size in between those by eROSITA and WFXT (see Comastri et al. 2010, this volume).

The identification of these objects will clearly require wide area surveys with deep multiband optical and near-IR imaging like e.g. the LSST surveys (Brusa et al. 2010, this volume). On the other hand, the WFXT surveys will represent a perfect complement for all optical and near-IR campaigns that search the unobscured part of the high-z AGN population as image dropouts. Late type brown dwarfs are the main contaminants in optically selected samples, being 15 times more abundant than high-z QSOs of comparable magnitudes (Fan et al. 2001). Even when using near-IR colors to separate them from high-z QSO candidates, the success rate of optical spectroscopy is only 20-30% (Jiang et al. 2009). If sensitive X-ray images were available underneath each optical dropout, a detection in the X-rays would almost automatically ensure that the object is an AGN, since brown dwarfs of comparable optical magnitudes are ~ 300 times fainter in the X-rays. LSST and WFXT surveys will then reinforce each other in the search of $z > 6$ AGN.

4. Evolution of the obscuration

A built-in feature of the BH/galaxy evolutionary sequence described in the Introduction is that an obscured accretion phase preceeds a clean accretion phase, at least in powerful, QSO-like objects. One may therefore wonder whether the fraction of obscured AGN was higher in the past. This indeed depends on many parameters such as i) the physical scale of the absorbing gas and how this is driven towards the BH; ii) the relative timescales of the obscured and unobscured phases; iii) whether the absorbed-to-unabsorbed AGN transition occurs also in low-mass/low-luminosity objects (i.e. Seyfert galaxies). Not many theoretical predictions on the evolution of the obscured AGN fraction are available in the literature. Models that relate the obscuration on nuclear scales to the availability of gas in the host galaxy generally predict an increase of the obscured AGN fraction with redshift (e.g Menci et al. 2008) since the gas mass in galaxies was larger in the past. Some others models, which anti-correlate the covering factor of the obscuring medium to the BH mass and then follow the evolution of the BH mass function using empirical relations (Lamastra et al. 2008), however do not predict such an increase. The situation is also debated from an observational point of view. An increase of the obscured AGN fraction with redshift among X-ray selected AGN has been observed by La Franca et al. (2005); Treister & Urry (2006); Hasinger (2008); Trump et al. (2009),

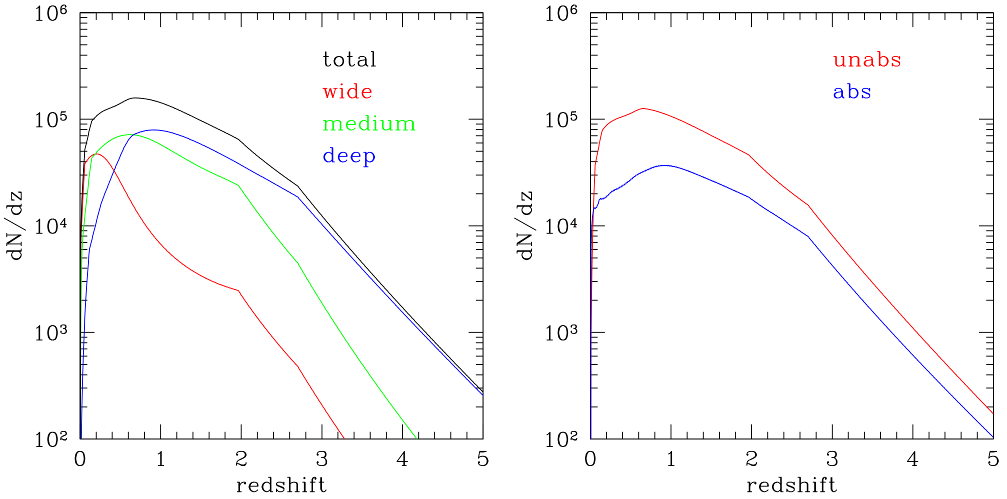

Fig. 4. *Left*: Redshift distribution of the 300,000 AGN with good X-ray spectra (i.e. with more than 1000 photons) in the three WFXT surveys. The Deep survey is providing most of the good X-ray spectra at $z > 1$. *Right*: As in the *left* panel but splitting the total sample of 300,000 AGN into unabsorbed ($\log N_H < 22$) and absorbed ($\log N_H \geq 22$) objects.

but other works did not find any evidence of this trend (Ueda et al. 2003; Dwelly & Page 2006; Gilli et al. 2007). Selection effects in these computations are very important and could mimic a spurious evolution of the obscured AGN fraction (see e.g. Gilli et al. 2010a).

Much of this uncertainty can be related to the lack of large statistical samples of AGN with high-quality X-ray spectra. Using samples of limited size, which cannot be split into narrow luminosity and redshift bins, it is often complicated to disentangle any redshift-dependent from luminosity-dependent effects (it is generally agreed that the obscured AGN fraction decreases with luminosity, but the slope and normalization of this relation differ from paper to paper). Furthermore, the absorption column density is often estimated either from the X-ray hardness ratio, or from the absence of broad emission lines in the optical spectrum. Both methods suffer from caveats and limitations (Brusa et al. 2010), and ideally the absorbing column should be measured through X-ray spectra with good photon statistics. The most recent XLF determinations contain $\lesssim$ 2000 AGN (Hasinger 2008; Silverman et al. 2008; Yencho et al. 2009; Ebrero et al. 2009; Aird et al. 2010), most of which are just slightly more than simple X-ray detections. With WFXT one would expect to detect about 300,000 AGN with good X-ray spectra, i.e. with more than 1000 photons each, in a broad redshift range ($z \sim 0-5$). As shown in Fig. 4 *left*, the WFXT-Deep survey is providing most of the good X-ray spectra at $z > 1$, while the Medium and Wide surveys provide the largest contribution at lower redshifts. About 1/3 of the detected objects with good X-ray spectra are expected to be absorbed by column densities above 10^{22} cm^{-2} (see Fig.4 *right*). Future wide area optical and near-IR surveys should provide redshifts, either spectroscopic or photometric, for a significant fraction of these sources, making possible to divide the sample into fine redshift, luminosity and obscuration bins and therefore map the cosmological evolution of nuclear obscuration.

5. The most obscured AGN

If the overall evolution of obscured AGN is uncertain, the evolution of the most heav-

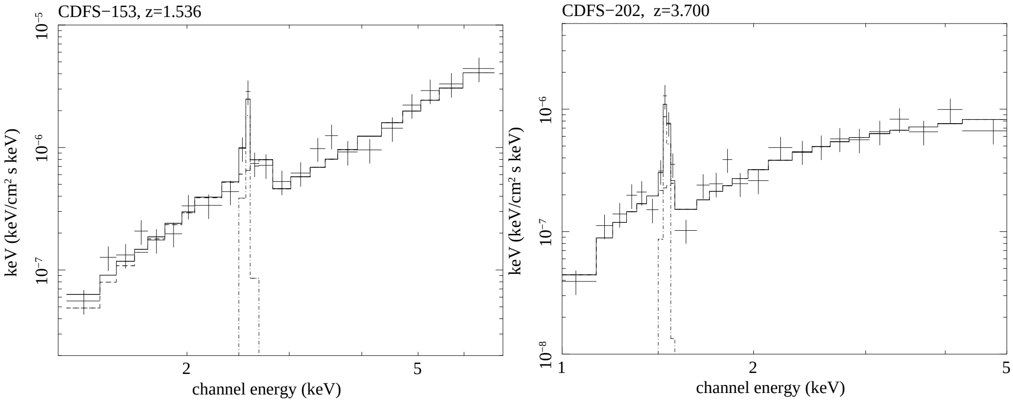

Fig. 5. Simulated WFXT spectra of CDFS-202 and CDFS-153, two high-z CT AGN with $f_{2-10} > 10^{-15}$ erg cm^{-2} s^{-1} observed in the XMM-CDFS: the goal effective area and an exposure time of 400 ks were assumed. No background is included, which however is not expected to alter significantly the S/N ratio (see text).The 100 deg^2 WFXT-Deep survey (Murray et al. 2008, Rosati et al. 2010, this volume) is expected to reveal about 500 objects like these at $z > 1$ in terms of obscuration and photon statistics.

ily obscured and elusive ones, the so-called Compton-Thick AGN ($N_H > 10^{24}$cm^{-2}; hereafter CT AGN), is completely unknown, making the census of accreting black holes largely incomplete.

Only ~50 *bona-fide* CT AGN, i.e. certified by X-ray spectral analysis, are known in the local Universe (Comastri 2004; Della Ceca et al. 2008), but their abundance has nonetheless been estimated to be comparable to that of less obscured ones (Risaliti et al. 1999). At higher redshifts, an integrated constrain to the space density of CT AGN can be obtained from the spectrum of the X-ray background. Depending on the assumptions, synthesis models of the XRB predict that from ~10 to ~30% of the XRB peak emission at 30 keV is produced by the emission of CT AGN integrated over all redshifts (Gilli et al. 2007; Treister et al. 2009), but the main contribution likely arises at $z \sim 1$. In the absence of any information, the luminosity function and evolution of CT AGN in XRB synthesis models have been usually assumed to be equal to those of less obscured ones. Because of the uncertainties in the average spectrum of CT AGN and in their evolution, however, the constraints to the CT space density from the XRB spectrum remain rather loose.

In recent years there have been many attempts to constrain the space density of CT AGN in different luminosity and redshift intervals exploiting different selection techniques. Very hard (> 10 keV) X-ray surveys are still limited in sensitivity and are just sampling the local Universe (Malizia et al. 2009). To sample AGN at higher redshifts, and in particular at $z \sim 1$, one needs to rely on deep X-ray surveys in the 2-10 keV band and try to select CT AGN either directly from X-ray spectroscopy, or by comparing the measured, obscured X-ray emission (if any) with some other indicator of the intrinsic nuclear power: IR selection can track the nuclear emission as reprocessed by the dusty absorber; narrow optical emission lines can sample the gas ionized by the nucleus on scales free from obscuration. X-ray stacking of IR-selected sources not individually detected in the X-rays has been used to estimate the space density of CT AGN at $z \sim 1 - 2$ (Daddi et al. 2007; Alexander et al. 2008; Fiore et al. 2009; Bauer et al. 2010). The comparison between the [O III]5007 and X-ray flux has been used to select X-ray underluminous QSOs and then estimate the density of CT QSOs at $z = 0.5$ (Vignali et al. 2010). To sample the population of CT around $z \sim 1$, Gilli et al. (2010b) recently devised a selection method based on the [Ne V]3426 emission line, which can be applied to optical spectroscopic surveys with deep X-ray coverage and seems to deliver clean, albeit not complete, samples of CT objects at $z > 0.8$, i.e. at redshifts not reachable with [O III]5007 selection. Despite these numerous efforts, [Ne V], [O III], and IR selection are all indirect ways to select CT AGN, since the CT nature of an object is simply inferred from the faintness of its X-ray emission relative to an indicator of the intrinsic power, and therefore may suffer from severe systematic uncertainties.

To unambiguously obtain samples of *bona-fide* CT AGN over a broad redshift range, very deep X-ray exposures are needed such as the 2.5 Ms XMM survey in the CDFS (Comastri et al. 2010, in prep.). A number of CT candidates, identified in the 1 Ms CDFS catalog on the basis of their flat (low quality) spectrum (Tozzi et al. 2006), are indeed being confirmed as such by the higher quality XMM spectra (Comastri et al. 2010, in prep.), including the well-known CT candidate CDFS-202 at $z = 3.7$ (Norman et al. 2002). Because of their limited sky coverage, however, only a few tens of *bona-fide* high-z CT AGN are expected to be detected in current deep X-ray surveys, making population studies of CT AGN problematic.

The WFXT surveys are expected to determine the cosmological evolution of *bona-fide* CT AGN up to $z \sim 3$. Based on the synthesis model by Gilli et al. (2007), the WFXT-Deep survey will return a sample of ∼ 500 objects at $z > 1$ which are *bona-fide* CT AGN, i.e. with more than 500 net counts in the 0.5-7 keV band (the number of simple detections of CT objects will be obviously much larger). In Fig. 5 we show two such objects (CDF-202 and CDFS-153, another CT AGN, at $z = 1.53$, found in the XMM-CDFS) simulated using the WFXT response matrices for the goal design. No background is assumed in the simulation, but, based on the level estimated for low-earth orbits (see Ettori & Molendi 2010, this volume), only about 20 background photons are expected above 1 keV, which would therefore not alter significantly the spectral quality. It is evident that 500 X-ray photons are sufficient to unambiguously reveal their CT nature: in principle, based on the iron Kα line, it would be possible to determine also their redshift without the need of optical spectroscopy. In total, 500, 270, 60 and 12 *bona-fide* CT AGN at redshifts above 1, 2, 3 and 4, respectively, are expected in the WFXT-Deep survey. Future missions sensitive to energies above 10 keV, such as NuSTAR and ASTRO-H (approved by NASA and JAXA, respectively) or EXIST and NHXM (proposed to NASA and ASI, respectively) are expected to allow population studies of CT AGN at $z < 1$, with a peak in the redshift distribution at $z \sim 0.3 - 0.4$. The WFXT mission appears to uniquely complement these and extend them to $z > 1$. Only IXO, on a longer timescale and depending on the adopted survey strategy and mission design, could possibly provide samples of distant CT objects matching in size those expected from WFXT.

6. Conclusions

About 15 millions of AGN in a very broad redshift and luminosity range will be detected by the WFXT surveys. Some of the major issues related to the evolution of accreting SMBHs are expected to be solved by this sample as detailed below.

- WFXT will break through the high-z Universe: more than 1600 AGN will be observed at $z > 6$, allowing population studies at these redshifts and providing an unvaluable complement for future wide area optical and near-IR surveys searching for black holes at the highest redshifts. Such a large sample is a unique feature of the WFXT surveys and cannot be matched by any other planned or proposed X-ray mission.

- Good X-ray spectra, with more than 1000 photons, will be obtained for 300,000 AGN allowing accurate measurements of their absorbing column density. This will make possible for the first time to measure the evolution of nuclear obscuration with cosmic time up to $z \sim 5$ and verify its connection with e.g. star formation.

- About 500 *bona fide*, i.e. certified by X-ray spectral analysis, CT AGN at $z > 1$ will be found in the WFXT-Deep survey. This will complement population studies at lower redshifts obtained by future high-energy surveys such as those performed by the approved missions NuSTAR and Astro-H and will make possible to detemine the abundance and evolution of this still missing BH population. Performing population studies of distant heavily obscured objects, and determining their relevance in the census of accreting black holes and evolutionaly path of galaxies is another unique science case to be carried out by WFXT.

Acknowledgements. We thank all the members of the WFXT collaboration. RG acknowledges stimulating discussions with R. Salvaterra. We acknowledge partial support from ASI-INAF and PRIN/MIUR under grants I/023/05/00, I/088/06/00 and 2006-02-5203.

References

Aird, J., Nandra, K., Laird, E. S., et al. 2010, MNRAS, 401, 2531
Alexander, D. M., Chary, R., Pope, A., et al. 2008, ApJ, 687, 835
Bauer, F. E., Yan, L., Sajina, A., & Alexander, D. M. 2010, ApJ, 710, 212
Beelen, A., Cox, P., Benford, D. J., et al. 2006, ApJ, 642, 694
Brusa, M., Civano, F., Comastri, A., et al. 2010, ApJ, 716, 348
Brusa, M., Comastri, A., Gilli, R., et al. 2009, ApJ, 693, 8
Comastri, A. 2004, in Astrophysics and Space Science Library, Vol. 308, Supermassive Black Holes in the Distant Universe, ed. A. J. Barger, 245–+
Cowie, L. L., Songaila, A., Hu, E. M., & Cohen, J. G. 1996, AJ, 112, 839
Daddi, E., Alexander, D. M., Dickinson, M., et al. 2007, ApJ, 670, 173
Della Ceca, R., Severgnini, P., Caccianiga, A., et al. 2008, Memorie della Societa Astronomica Italiana, 79, 65
Dwelly, T. & Page, M. J. 2006, MNRAS, 372, 1755
Ebrero, J., Carrera, F. J., Page, M. J., et al. 2009, A&A, 493, 55
Elvis, M., Civano, F., Vignali, C., et al. 2009, ApJS, 184, 158
Fan, X. 2006, New Astronomy Review, 50, 665
Fan, X., Narayanan, V. K., Lupton, R. H., et al. 2001, AJ, 122, 2833
Feruglio, C., Maiolino, R., Piconcelli, E., et al. 2010, A&A, 518, L155+
Fiore, F., Puccetti, S., Brusa, M., et al. 2009, ApJ, 693, 447
Gilli, R., Comastri, A., & Hasinger, G. 2007, A&A, 463, 79
Gilli, R., Comastri, A., Vignali, C., Ranalli, P., & Iwasawa, K. 2010a, in American Institute of Physics Conference Series, Vol. 1248, American Institute of Physics Conference Series, ed. A. Comastri, L. Angelini, & M. Cappi, 359–364
Gilli, R., Vignali, C., Mignoli, M., et al. 2010b, A&A, 519, A92+
Hasinger, G. 2008, A&A, 490, 905
Hasinger, G., Miyaji, T., & Schmidt, M. 2005, A&A, 441, 417
Hopkins, P. F., Hernquist, L., Cox, T. J., & Kereš, D. 2008, ApJS, 175, 356
Jiang, L., Fan, X., Bian, F., et al. 2009, AJ, 138, 305
Jiang, L., Fan, X., Brandt, W. N., et al. 2010, Nature, 464, 380
Juarez, Y., Maiolino, R., Mujica, R., et al. 2009, A&A, 494, L25
Kauffmann, G. & Haehnelt, M. 2000, MNRAS, 311, 576
Kurk, J. D., Walter, F., Fan, X., et al. 2009, ApJ, 702, 833
Kurk, J. D., Walter, F., Fan, X., et al. 2007, ApJ, 669, 32
La Franca, F., Fiore, F., Comastri, A., et al. 2005, ApJ, 635, 864
Lamastra, A., Menci, N., Maiolino, R., Fiore, F., & Merloni, A. 2010, MNRAS, 405, 29
Lamastra, A., Perola, G. C., & Matt, G. 2008, A&A, 487, 109
Lehnert, M. D., Nesvadba, N. P. H., Cuby, J., et al. 2010, Nature, 467, 940
Li, Y., Hernquist, L., Robertson, B., et al. 2007, ApJ, 665, 187
Luo, B., Bauer, F. E., Brandt, W. N., et al. 2008, ApJS, 179, 19

Madau, P. & Rees, M. J. 2001, ApJ, 551, L27
Malizia, A., Stephen, J. B., Bassani, L., et al. 2009, MNRAS, 399, 944
Marconi, A., Risaliti, G., Gilli, R., et al. 2004, MNRAS, 351, 169
Marulli, F., Bonoli, S., Branchini, E., Moscardini, L., & Springel, V. 2008, MNRAS, 385, 1846
Menci, N., Fiore, F., Puccetti, S., & Cavaliere, A. 2008, ApJ, 686, 219
Monaco, P., Fontanot, F., & Taffoni, G. 2007, MNRAS, 375, 1189
Murray, S. S., Kenter, A., Forman, W. R., et al. 2005, ApJS, 161, 1
Murray, S. S., Norman, C., Ptak, A., et al. 2008, in Society of Photo-Optical Instrumentation Engineers (SPIE) Conference Series, Vol. 7011, Society of Photo-Optical Instrumentation Engineers (SPIE) Conference Series
Narayanan, D., Li, Y., Cox, T. J., et al. 2008, ApJS, 174, 13
Norman, C., Hasinger, G., Giacconi, R., et al. 2002, ApJ, 571, 218
Oesch, P. A., Bouwens, R. J., Illingworth, G. D., et al. 2010, ApJ, 709, L16
Rhook, K. J. & Haehnelt, M. G. 2008, MNRAS, 389, 270
Richards, G. T., Strauss, M. A., Fan, X., et al. 2006, AJ, 131, 2766
Risaliti, G., Maiolino, R., & Salvati, M. 1999, ApJ, 522, 157
Salvaterra, R., Della Valle, M., Campana, S., et al. 2009, Nature, 461, 1258
Salvaterra, R., Haardt, F., & Volonteri, M. 2007, MNRAS, 374, 761
Shankar, F., Salucci, P., Granato, G. L., De Zotti, G., & Danese, L. 2004, MNRAS, 354, 1020
Silverman, J. D., Green, P. J., Barkhouse, W. A., et al. 2008, ApJ, 679, 118
Taniguchi, Y. 2008, in IAU Symposium, Vol. 250, IAU Symposium, ed. F. Bresolin, P. A. Crowther, & J. Puls, 429–436
Tanvir, N. R., Fox, D. B., Levan, A. J., et al. 2009, Nature, 461, 1254
Tozzi, P., Gilli, R., Mainieri, V., et al. 2006, A&A, 451, 457
Treister, E. & Urry, C. M. 2006, ApJ, 652, L79
Treister, E., Urry, C. M., & Virani, S. 2009, ApJ, 696, 110
Trump, J. R., Impey, C. D., Elvis, M., et al. 2009, ApJ, 696, 1195
Ueda, Y., Akiyama, M., Ohta, K., & Miyaji, T. 2003, ApJ, 598, 886
Vignali, C., Alexander, D. M., Gilli, R., & Pozzi, F. 2010, MNRAS, 404, 48 (V10)
Volonteri, M., Lodato, G., & Natarajan, P. 2008, MNRAS, 383, 1079
Walter, F., Carilli, C., Bertoldi, F., et al. 2004, ApJ, 615, L17
Wilkins, S. M., Bunker, A. J., Ellis, R. S., et al. 2010, MNRAS, 403, 938
Willott, C. J., Delorme, P., Reylé, C., et al. 2009, AJ, 137, 3541
Willott, C. J., Delorme, P., Reylé, C., et al. 2010, AJ, 139, 906
Yencho, B., Barger, A. J., Trouille, L., & Winter, L. M. 2009, ApJ, 698, 380